U.S. Department of the Interior
U.S. Geological Survey

Open-File Report 2010–1083–J
Version 1.1, revised January 28, 2014

Seismicity of the Earth 1900–2010

Himalaya and Vicinity

Compiled by Bethan Turner,[1] Jennifer Jenkins,[1] Rebecca Turner,[1] Amy L. Parker,[1] Alison Sinclair,[1] Sian Davies,[1] Gaven P. Hayes,[2] Antonio Villaseñor,[3] Richard L. Dart,[2] Arthur C. Tarr,[2] Kevin P. Furlong,[4] and Harley M. Benz[2]
2013

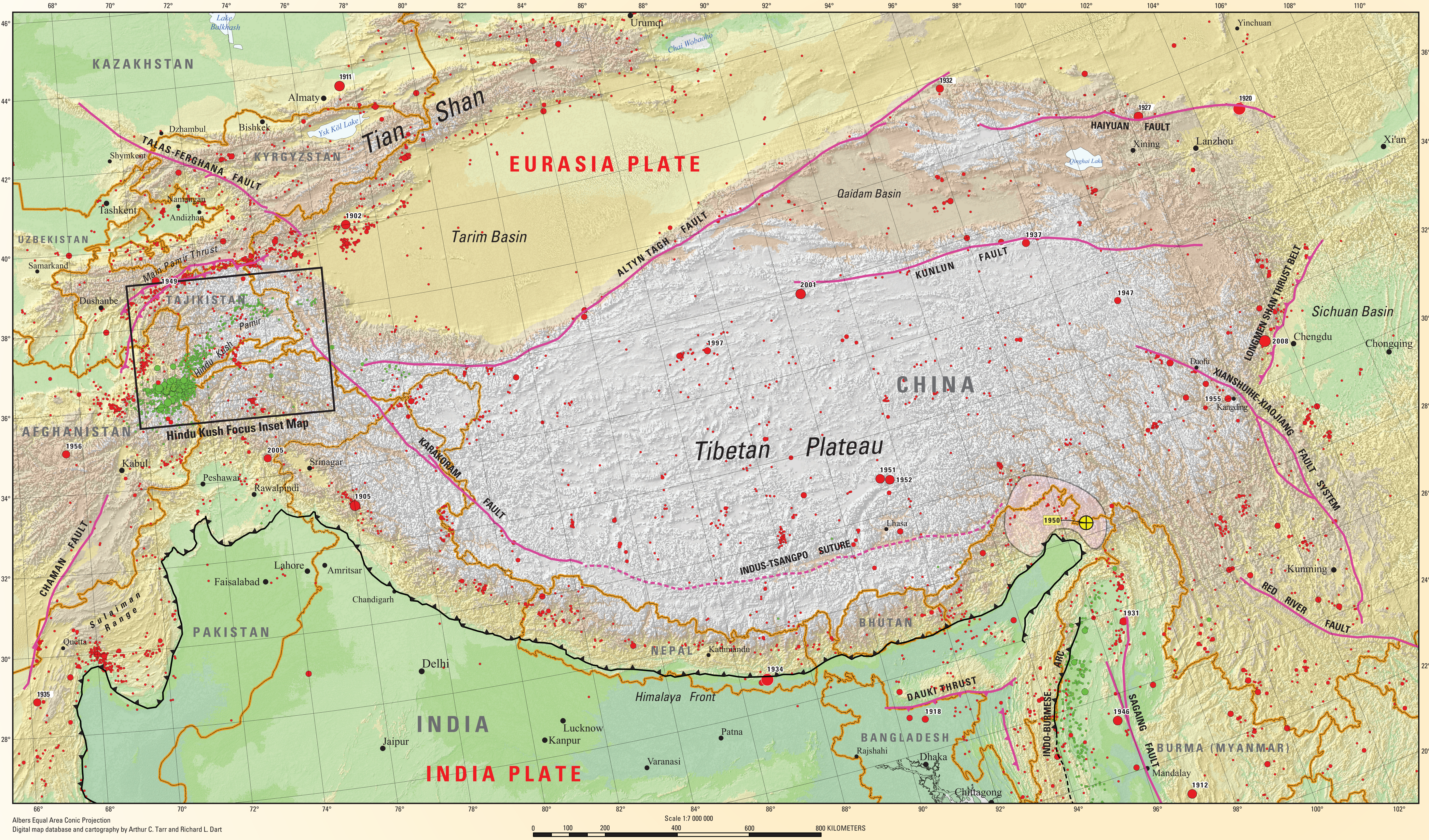

MAP EXPLANATION

Magnitude classes: 5.5–5.9, 6–6.4, 6.5–6.9, 7–7.4, 7.5, 7.6, 7.7, 7.8, 7.9, 8.0, 8.1, 8.2

Depth of focus: 0–69 km; 70–299 km; 300–700 km

Nucleation points

Rupture zones

Plate boundaries: Subduction; Transform; Divergent; Others

Large Active Fault

Suture

Country Boundary

TECTONIC SUMMARY

Seismicity in the Himalaya primarily results from the continental collision of the India and Eurasia plates, which are converging at a relative rate of 40–50 mm/yr. Approximately half of this convergence is accommodated across the Himalaya. Northward underthrusting of India beneath Eurasia generates numerous earthquakes and consequently makes this area one of the most seismically hazardous regions on Earth. The surface expression of the plate boundary is marked by the foothills of the north-south trending Sulaiman Range in the west, the Indo-Burmese Arc in the east and the east-west trending Himalaya Front in the north of India.

The India-Eurasia plate boundary is a diffuse boundary, which in the region near the north of India, lies within the limits of the Indus-Tsangpo (also called the Yarlung-Zangbo) Suture Zone to the north and the Main Frontal Thrust to the south. The Indus-Tsangpo Suture Zone is located roughly 200 km north of the Himalaya Front and is defined by an exposed ophiolite chain along its southern margin. The narrow (<200 km) Himalaya Front includes numerous east-west trending, parallel structures. This region has the highest rates of seismicity and largest earthquakes in the Himalaya region, caused mainly by movement on thrust faults. Examples of significant earthquakes, in this densely populated region, caused by reverse-slip movement include the 1934 M8.1 Bihar, the 1905 M7.5 Kangra, and the 2005 M7.6 Kashmir earthquakes. The latter two resulted in the highest death tolls for Himalaya earthquakes seen to date, together killing over 100,000 people and leaving millions homeless. The largest instrumentally recorded Himalaya earthquake occurred on 15 August 1950 in Assam, eastern India. This M8.6 right-lateral, strike-slip earthquake was widely felt over a broad area of central Asia, causing extensive damage to villages in the epicentral region.

The Tibetan Plateau is situated north of the Himalaya, stretching approximately 1,000 km north-south and 2,500 km east-west, and is geologically and tectonically complex with several sutures which are hundreds of kilometers long and generally trend east-west. The Tibetan Plateau is cut by a number of large (>1,000 km) east-west trending left-lateral strike-slip faults, including the Kunlun, Haiyuan, and the Altyn Tagh. Right-lateral strike-slip faults (comparable in size to the left-lateral faults) in this region include the Karakorum, Red River, and Sagaing. Secondary north-south trending normal faults also cut the Tibetan Plateau. Thrust faults are found towards the north and south of the Tibetan Plateau. Collectively, these faults accommodate crustal shortening associated with the ongoing collision of the India and Eurasia plates, with thrust faults accommodating north-south compression, and normal and strike-slip faults accommodating east-west extension.

Along the western margin of the India plate, in the vicinity of southeastern Afghanistan and western Pakistan, the India plate translates obliquely relative to the Eurasia plate, resulting in a complex fold-and-thrust belt known as the Sulaiman Range. Faulting in this region includes strike-slip, reverse-slip and oblique-slip motion and often results in shallow, destructive earthquakes. The active, left-lateral, strike-slip Chaman fault is the fastest moving fault in the region. In 1505, a segment of the Chaman fault near Kabul, Afghanistan, ruptured causing widespread destruction. In the same region the more recent 30 May 1935, M7.6 Quetta earthquake, which occurred in the Sulaiman Range in Pakistan, killed as many as 35,000 people.

On the northwestern side of the Tibetan Plateau, beneath the Pamir–Hindu Kush Mountains of northern Afghanistan, earthquakes occur at depths as great as 200 km as a result of remnant lithospheric subduction (see cross sections). Shallow crustal earthquakes also occur in this region near the Main Pamir Thrust and other active Quaternary faults. The Main Pamir Thrust, north of the Pamir Mountains, is an active shortening structure. The northern portion of the Main Pamir Thrust produces many shallow earthquakes, whereas its western and eastern borders display a combination of thrust and strike-slip mechanisms (Fan and others, 1994). On the 18 February 1911, the M7.4 Sarez earthquake ruptured in the Central Pamir Mountains, killing numerous people and triggering a landside, which blocked the Murghab River.

Further north, the Tian Shan is a seismically active intra-continental mountain belt, which extends 2,500 km in an ENE-WNW orientation north of the Tarim Basin. This belt is defined by numerous east-west trending thrust faults, creating a compressional basin-and-range landscape. It is generally thought that regional stresses associated with the collision of the India and Eurasia plates are responsible for faulting in the region. The region has had three major earthquakes (>M7.6) at the start of the 20th Century, including the 1902 Atushi earthquake,which killed an estimated 5,000 people. The range is cut through in the west by the 700-km-long, northwest-southeast striking, Talas-Ferghana active right-lateral, strike-slip fault system. Though the system has produced no major earthquakes in the last 250 years, paleoseismic studies indicate that it has the potential to produce M7.0+ earthquakes and it is thought to represent a significant hazard (Burtmen and others,1996).

The northern portion of the Tibetan Plateau itself is largely dominated by the motion on three large left-lateral, strike-slip fault systems: the Altyn Tagh, Kunlun and Haiyuan. The Altyn Tagh fault is the longest of these strike-slip faults and it is thought to accommodate a significant portion of plate convergence. However, this system has not undergone significant historical earthquakes, though paleoseismic studies show evidence of prehistoric M7.0–8.0 events (Washburn and others, 2001). Thrust faults link with the Altyn Tagh at its eastern and western termini. The Kunlun Fault, south of the Altyn Tagh, is seismically active, producing large earthquakes such as the 8 November 1997, M7.6 Manyi earthquake and the 14 November 2001, M7.8 Kokoxili earthquake. The Haiyuan fault, in the far northeast, generated the 16 December 1920, M7.8 earthquake that killed approximately 200,000 people and the 22 May 1927, M7.6 earthquake that killed 40,912.

The Longmen Shan thrust belt, along the eastern margin of the Tibetan Plateau, is an important structural feature and forms a transitional zone between the complexly deformed Songpan-Garze Fold Belt and the relatively undeformed Sichuan Basin. On 12 May 2008, the thrust belt produced the reverse slip, M7.9 Wenchuan earthquake, killing over 87,000 people and causing the equivalent of billions of U.S. dollars in damages and landslides, which dammed several rivers and lakes.

Southeast of the Tibetan Plateau are the right-lateral, strike-slip Red River and the left-lateral, strike-slip Xianshuihe-Xiaojiang fault systems. The Red River Fault underwent large scale, left-lateral ductile shear during the Tertiary period before changing to its present day right-lateral slip rate of approximately 5 mm/yr (Replumaz and others, 2001). This fault has produced several earthquakes >M6.0 including the 4 January 1970, M7.5 earthquake in Tonghai which killed over 10,000 people. Since the start of the 20th century, the Xianshuihe-Xiaojiang Fault system has generated several M7.0+ earthquakes including the M7.5 Luhuo earthquake which ruptured on 22 April 1973 (Allen and others, 1991). Some studies suggest that due to the high slip rate on this fault, future large earthquakes are highly possible along the 65 km stretch between Daofu and Qianning and the 135 km stretch that runs through Kangding.

Shallow earthquakes within the Indo-Burmese Arc, predominantly occur on a combination of strike-slip and reverse faults, including the Sagaing, Kabaw, and Dauki faults. Between 1930 and 1956, six M7.0+ earthquakes occurred near the right-lateral Sagaing Fault, resulting in severe damage in Burma including the generation of landslides, liquefaction and the loss of 610 lives. Deep earthquakes (>200 km) have also been known to occur in this region, these are thought to be due to the subduction of the eastwards-dipping India plate, though whether subduction is currently active is debated. Within the pre-instrumental period, the large Shillong earthquake occurred on 12 June 1897, causing widespread destruction.

DATA SOURCES

The earthquake locations shown on the main map (above) and on the depth profiles (right) are taken from the global 1900–2007 Centennial catalog (Engdahl and Villaseñor, 2002), a catalog of high-quality depth determinations for the period 1964–2002 (Engdahl, personal commun., 2003), and USGS-PDE (Preliminary Determination of Epicenters) for the years 2008–2010. Major earthquakes (7.5≤M≤8.2) are labeled with the year of occurrence, while earthquakes (8.0≤M≤8.2) are labeled with the year of occurrence and also denoted by a white outline (Tarr and others, 2010).

The nucleation points of great earthquakes (M≥8.3) are designated with a label showing the year of occurrence. Their rupture areas are shown as pink polygons. Major earthquakes (7.5≤M≤8.2) are labeled with the year of occurrence.

The Seismic Hazard and Relative Plate Motion panel displays the generalized seismic hazard of the region (Giardini and others, 1999) and representative relative plate-motion vectors using the Morvel model (DeMets and others, 1994).

Base map data sources include GEBCO 2008 shaded relief, Volcanoes of the World dataset (Siebert and Simkin, 2002), plate boundaries (Bird, 2003), and geographic information from Digital Chart of the World (1992), and ESRI (2002).

Hindu Kush Focus Inset Map

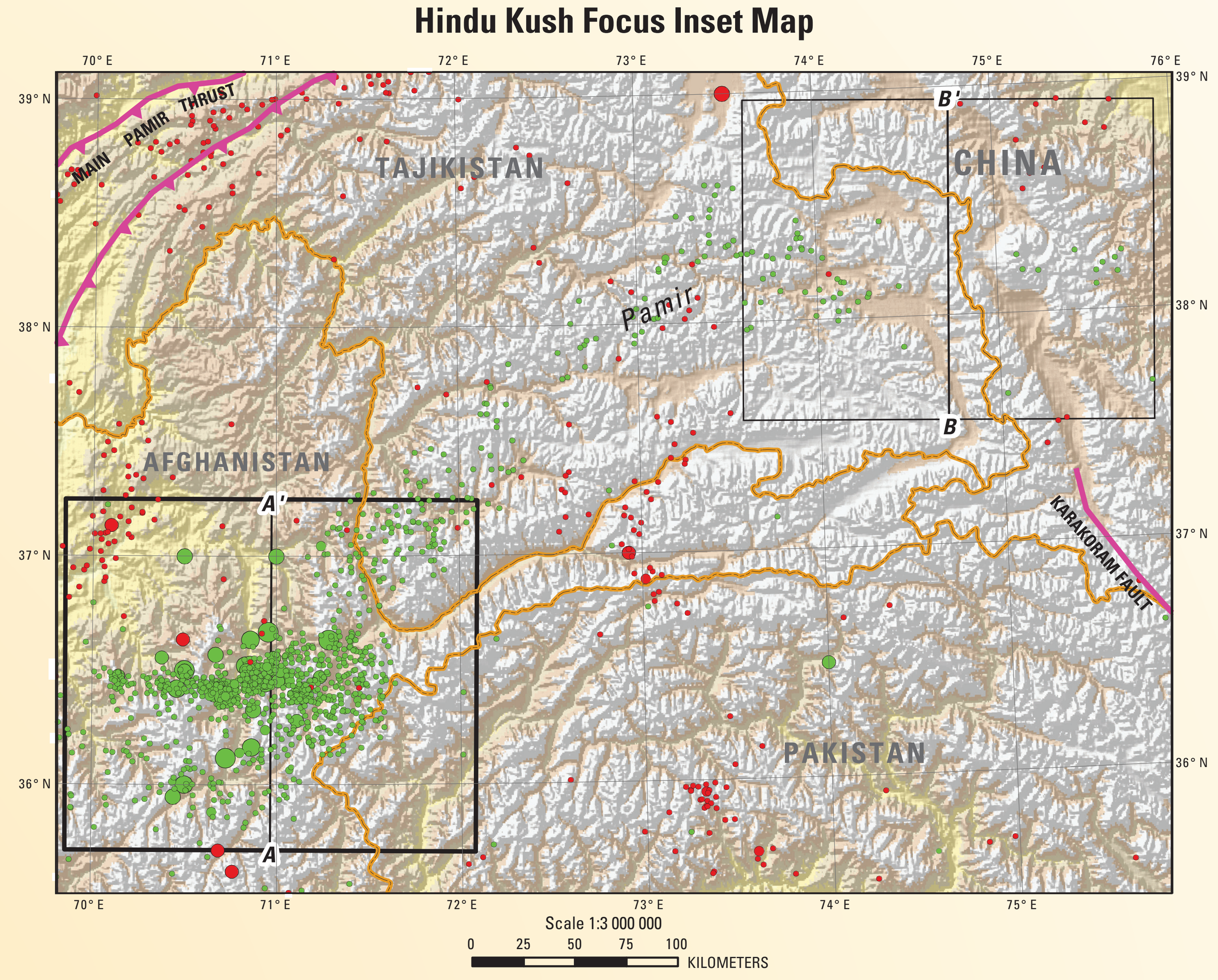

The curved arc of deep earthquakes found in the Hindu Kush–Pamir region indicates the presence of a lithospheric body at depth,thought to be remnants of a subducting slab. The cross section through the Hindu Kush region suggests a near vertical, northerly dipping subducting slab (cross section ***A***), whereas the cross section through the nearby Pamir region to the east indicates a much shallower dipping, southerly subducting slab (cross section ***B***). Some models suggest the presence of two subduction zones with the Indian plate being subducted beneath the Hindu Kush region, and the Eurasian plate being subducted beneath the Pamir region. However, other models suggest that just one of the twoplates is being subducted and that the slab has become contorted and overturned in places.

DEPTH PROFILE EXPLANATION

Profiles of earthquake and volcanoes are constructed from the mapped data. Locations of the profile intersection with the surface are drawn in the map and labeled to coincide with the profile label. Box defines extent of earthquakes included in the profile. Length of the profile graphic is the same as in the map. Distance in kilometers from the trench axis is indicated in the X direction, depth in kilometers is indicated in the Y direction. There is no vertical exaggeration. See Explanation color key. Not all earth layers, earthquake depths or magnitude, are visible on every profile.

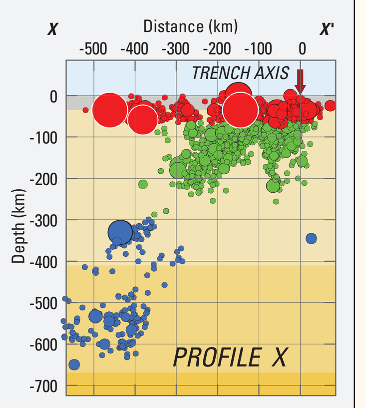

Magnitude: 4–5.9, 6–6.4, 6.5–6.9, 7–7.4, 7.5, 7.6, 7.7, 7.8, 7.9, 8.0, 8.1, 8.2

Depth of focus: 0–69 km; 70–299 km; 300–700 km

Earth structure: Air; Crust; Upper mantle; Transition zone; Lower mantle

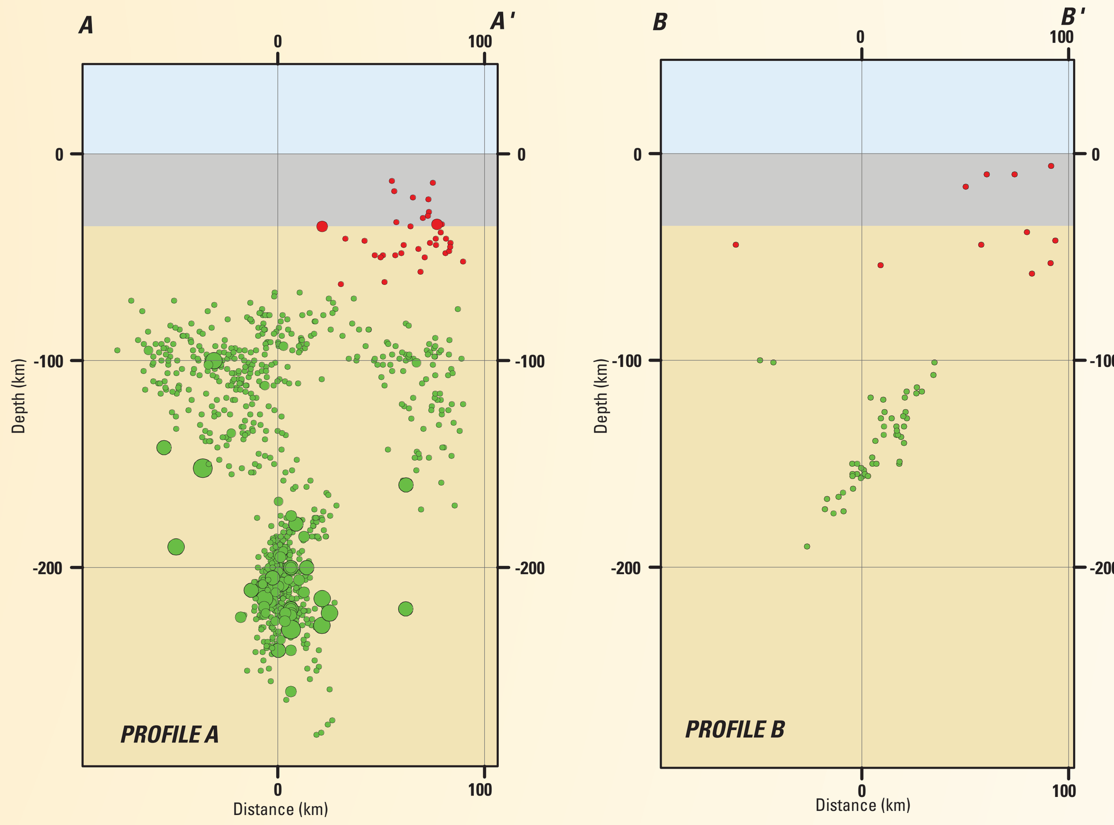

Seismic Hazard and Relative Plate Motion

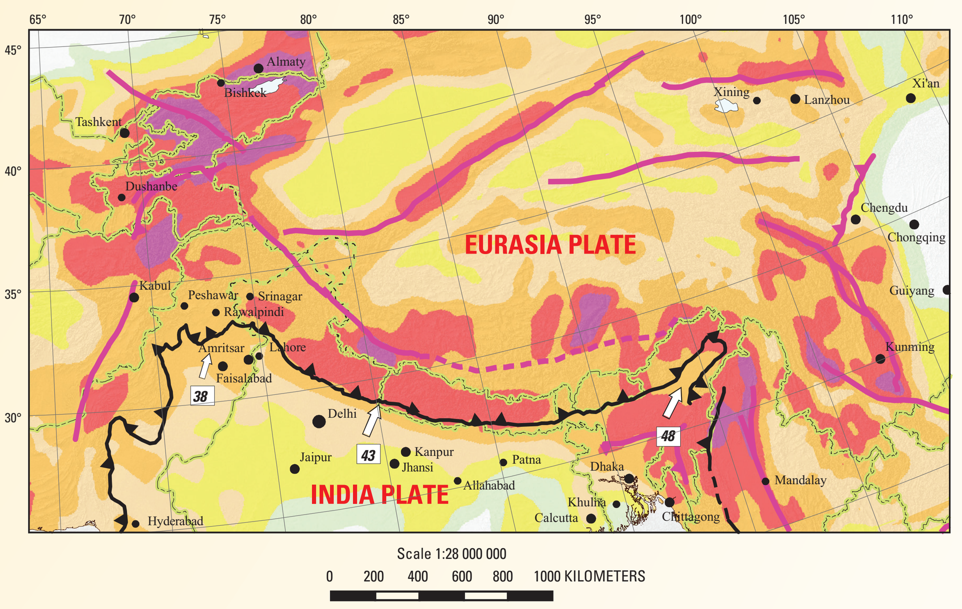

FIGURE EXPLANATION

Peak ground acceleration: 0–0.2 m/s²; 0.2–0.4; 0.4–0.8; 0.8–1.6; 1.6–3.2; 3.2–6.4; 6.4–9.8

Plate boundaries: Subduction; Transform; Divergent; Others

Relative plate motion in mm/yr: 43

Large Active Fault

Suture

Country Boundary

REFERENCES

Allen, C.R. Zhuoli, L., Hong, Q., Xueze, W., Huawei, Z., Weishi, H.,1991, Field study of a highly active fault zone—The Xianshuihe fault of southwestern China: Geological Society of America Bulletin, v. 103, p. 1178–1199.

Ambraseys, Nicholas, and Bilham, Roger, 2003, Earthquakes and crustal deformation in northern Baluchistan: Bulletin of the Seismological Society of America, v. 93, no. 4, p. 1573–1605.

Bilham, Roger, Larson, K., Freymueller, J., and Project Idylhim members, 1997, GPS measurements of present-day convergence across the Nepal Himalaya: Nature (London), v. 386, p. 61–64.

Billington, S., Isacks, B.I., Barazangi, M., 1977, Spatial and focal mechanisms of mantle earthquakes in the Hindu Kush–Pamir region—A contorted Benioff zone: Geology, v. 5, p. 699–704.

Bird, Peter, 2003, An updated digital model of plate boundaries: Geochemistry Geophysics Geosystems, v. 4, no. 3, 52 p.

Burtmen, V.S, Skobelev, S.F., Molnar, P., 1996, Late Cenozoic slip on the Talas-Ferghana fault, the Tien Shan, central Asia: Geological Society of America Bulletin, v. 108, no. 8, p. 1004–1021.

Cavalié, O., Lasserre, C., Doin, M.P., Peltzer, G., Sun, J., Xu, X., Shen, Z.-K., 2008, Measurement of interseismic strain across the Haiyuan fault (Gansu, China), by In SAR: Earth and Planetary Science Letters, v. 275, p. 246–257.

Chen, W.-P. and Molnar, P., 1977, Seismic moments of major earthquakes and the average rate of slip in Central Asia: Journal of Geophysical Research, v. 82, p. 2945–2969.

Chen, S.F., Wilson, C.J.L., 1995, Emplacement of the Longmen Shan Thrust–Nappe Belt along the eastern margin of the Tibetan Plateau: Journal of Structural Geology, v. 18, p. 413–430.

Cowgill, E., Yin, A., Wang, X.F., and Zhang, Q., 2000, Is the North Altyn fault part of a strike-slip duplex along the Altyn Tagh fault system?: Geology, v. 28, no. 3, p. 255–258.

Daëron, M., Klinger, Y., Tapponnier, P., Elias, A., Jacques, E., and Sursock, A., 2005, Sources of the large A.D. 1202 and 1759 Near East earthquakes: Geology, v. 35, p. 755–758, doi:10.1130/G23631A.1.

DeMets, Charles, Gordon, R.G., Argus, D.F., and Stein, Seth, 1994, Effects of recent revisions to the geomagnetic time scale on estimates of current plate motions: Geophysical Research Letters, v. 21, p. 2191–2194.

Digital Chart of the World, 1992: Accessed July 5, 2012, at *http://earth-info.nga.mil/publications/specs/printed/89009/89009_DCW.pdf*.

Engdahl, E.R., and Villaseñor, Antonio, 2002, Global seismicity 1900–1999, *in* Lee, W.H.K., Kanamori, Hiroo, Jennings, P.C., and Kisslinger, Carl, eds., International Handbook of Earthquake and Engineering Seismology, v. 81(A), chap. 41, p. 1–26.

ESRI, 2002, ESRI data and maps: Redlands, Calif., ESRI, *http://www.esri.com/data/data-maps*.

Fan, G., Ni, J.F., Wallace, T.C., 1994, Active tectonics of the Pamirs and Karakorum: Journal of Geophysical Research, v. 99, p. 7131–7160.

GEBCO, 2008, The GEBCO_08_Grid, ver. 20091120: GEBCO. Accessed July 5, 2012, at *http://www.gebco.net*.

Giardini, D., Grünthal, G., Shedlock, K., Zhang, P., and Global Seismic Hazards Program, 1999, Global Seismic Hazards Map: Accessed on July 5, 2012, at *http://www.seismo.ethz.ch/static/GSHAP/*.

Hubbard, J., Shaw, J.H., 2009, Uplift of the Longmen Shan and Tibetan plateau, and the 2008 Wenchuan (M = 7.9) earthquake: Nature, v. 458, p. 194–197.

National Oceanic and Atmospheric Administration (NOAA), 2010: National Geophysical data Center (NGDC): National Oceanic and Atmospheric Administration, Accessed on Mar. 31, 2010, at *http://www.ngdc.noaa.gov/ngdc.html*.

Negredo, A.M., Replumaz, Ann, Villaseñor, Antonio, Guillot, Stéphane, 2007, Modeling the evolution of continental subduction processes in the Pamir–Hindu Kush region: Earth and Planetary Science Letters, v. 259, issues 1–2, p. 212–225.

Replumaz, Ann, Lacassin, R., Tapponier, P., Leloup, P.H., 2001, Large river offsets and Plio-Quaternary dextral slip rate on the Red River fault (Yunnan, China): Journal of Geophysical Research, v. 106, p. 819–836.

Siebert, Lee, and Simkin, Thomas, 2002, Volcanoes of the world—An illustrated catalog of Holocene volcanoes and their eruptions: Smithsonian Institution, Global Volcanism Program Digital Information Series, GVP-3. Accessed on Jan. 9, 2007, at *http://www.volcano.si.edu/world*

Szeliga, W.R., Bilham, Roger, Kakar, D.M., and Lodi, Sarosh, 2012, Interseismic strain accumulation along the western boundary of the Indian subcontinent: Journal of Geophysical Research, v. 117, B08404, doi:10.1029/2011JB008822.

Tarr, A.C., Villaseñor, Antonio, Furlong, K.P., Rhea, Susan, and Benz, H.M., 2010, Seismicity of the Earth 1900–2007: U.S. Geological Survey Scientific Investigations Map 3064, scale 1:25,000,000.

Washburn, Zachary, Arrowmith, J.R., Forman, S.L., Cowgill, Eric, Xiaofeng, Wang, Yueqiao, Zhang, Zhengel, Chen, 2001, Late Holocene earthquake history of the central Altyn Tagh fault, China: Geology, v. 29, no. 11, p. 1051–1054.

[1]Department of Earth and Ocean Sciences, University of Liverpool, Liverpool, United Kingdom
[2]U.S. Geological Survey
[3]Institute of Earth Sciences, CSIC, Barcelona, Spain
[4]Department of Geosciences, Pennsylvania State University, State College, PA, United States

Publishing support provided by:
Denver Publishing Service Center

Manuscript approved on February 10, 2013

Any use of trade, product or firm names is for descriptive purposes only and does not imply endorsement by the U.S. Government.

Although this information product, for the most part, is in the public domain, it also contains copyrighted materials as noted in the text. Permission to reproduce copyrighted items must be secured from the copyright owner.

Suggested citation:
Turner, Bethan, Jenkins, Jennifer, Turner, Rebecca, Parker, A.L., Sinclair, Alison, Davies, Sian, Hayes, G.P., Villaseñor, Antonio, Dart, R.L., Tarr, A.C., Furlong, K.P., and Benz, H.M., 2013, Seismicity of the Earth 1900–2010 Himalaya and vicinity (ver. 1.1, Jan. 28, 2014): U.S. Geological Survey Open-File Report 2010–1083–J, scale 1:9,000,000, *http://pubs.usgs.gov/of/2010/1083/j*.

This and other USGS information products are available at *http://store.usgs.gov/*.
U.S. Geological Survey
Box 25286, Denver Federal Center
Denver, CO 80225

To learn about the USGS and its information products visit *http://www.usgs.gov/*.
1-888-ASK-USGS

This report is available at:
http://pubs.usgs.gov/of/2010/1083/J

For more information concerning this publication, contact:
Center Director, USGS Geologic Hazards Science Center
Box 25046, Mail Stop 966
Denver, CO 80225
(303) 273-8579

Or visit Geologic Hazards Science Center Web site at:
http://geohazards.cr.usgs.gov/